

MRI detects in vivo migration of rat's bone marrow derived mesenchymal stem cells towards quinolinic acid lesion

N. Shemesh¹, O. Sadan^{2,3}, D. Offen^{2,3}, E. Melamed^{2,3}, and Y. Cohen¹

¹School of Chemistry, Tel Aviv University, Tel Aviv, Israel, ²Laboratory of Neurosciences, FMRC, Rabin Medical Center, Tel Aviv, Israel, ³Sackler School of Medicine, Tel Aviv University, Tel Aviv, Israel

Introduction

Huntington's disease (HD) is a hereditary neurodegenerative disease characterized by a progressive degeneration of the striatum. A striatal injection of quinolinic acid (QA) produces a striatal lesion that has similar pathological characteristics as found in the striatum of HD patients; therefore QA is an important animal model in studying HD (1). Stem cells hold a great promise for treatment of neurodegenerative diseases such as Parkinson's disease (PD), and HD (2). The use of mesenchymal stem cells (MSCs) that can differentiate to CNS like cells bypasses the ethical complications of embryonic stem cells (ESCs) production. This makes MSCs candidates for the treatment of CNS related diseases. One of the major *caveats* of stem cell transplantations is the fate of the transplanted cells. Once transplanted, it is difficult to determine cell viability in a non-invasive manner, or to delineate the transplanted cells from host tissue. Following the migration of super-paramagnetic iron oxide (SPIO) labeled stem cells can provide an indirect evidence for cell viability (3) since their migration ability stems from their ability to follow chemotactic signals that are sent outward by the lesion. Therefore, the goal of this study was to harness MRI to demonstrate that our differentiated MSCs are viable post-transplantation in the QA model of HD, and that they can migrate towards the lesion.

Materials and Methods

Mesenchymal stem cells were obtained from the femur and tibia of Wistar rats. In the second to fifth passage the cells were treated for a week with a unique differentiation medium, consisting of N2, epidermal, platelet derived and fibroblast growth factors (GF), isobutylmethylxanthine and cyclic AMP. The differentiated cells secrete several growth factors, among them vasoendothelial (VEGF) and brain derived neurotrophic factor (BDNF). The cells were pre-labeled using the PKH-26 fluorescent dye (Sigma) and exposed to 5µg/ml medium of SPIO nanoparticles (Ferridex) along with 1µg/ml poly-L-lysine overnight (3). Wistar rats (N=9) 3 months of age, W=250±20gr were anaesthetized with an i.p. injection of 0.5ml/100gr of 7% chloral hydrate and placed on a stereotaxic device. 250nmol in 1µL of QA [Sigma] was injected to the striatum. MSCs (~2.5E5) were transplanted posterior to the QA lesion (N=6). Control rats (N=3) were transplanted with 5µg SPIO particles in 1µL.

MRI- Anesthesia was induced with 4% isoflurane in 95% O₂, and maintained with ~1% isoflurane at a flow rate of ~1l/min. Respiratory rate was monitored throughout the experiments. Body temperature was maintained by circulating water in 37°C. MRI scans were performed on a 7.0T/30cm Bruker Biospec equipped with a gradient system capable of producing gradient pulses of 400mT/m. A body coil was used as the transmit coil, and a rat quadrature coil was used as the receiving coil. MRI experiments were performed at 0, 3, 8 and 18 days post transplantation and QA injection. Scans included: 2D GE images (FLASH, TR/TE=750/20ms, flip angle=30°) and T₂WI RARE8 (TR/TE=3500/75ms). For both scans the FOV was 2.56x2.56, the matrix size was 256x128 zero filled to 256x256, and a slice thickness of 700µm was chosen. In addition, 3D slab GEFI images (FLASH, TR/TE=150/14ms, flip angle=15°) FOV=2.56x2.56x0.48cm, matrix size=128x96x24 zero filled to 128x128x32 resulting in a spatial resolution of 200x200x150(µm)³ or with a matrix size of 256x128x64 zero filled to 256x256x64 resulting in a spatial resolution of 100x100x75(µm)³ were collected.

Histology- On the 19th day the animals were perfused intracardially with PBS following 4% paraformaldehyde. The brain tissue was removed, fixed and frozen. The tissues were cryosectioned into axial 10µm sections. Tissue sections were blocked using 5% goat serum and immunostained for astrocytic markers (αS100β) and macrophage marker (αCD 68).

Results

The progression of the lesion is depicted in Fig. 1 (Panels A, B days 0, 18 post QA injection respectively). The initial edema progresses until day 3 (data not shown), then subsides to leave a pronounced striatal lesion at day 18. The 2D GE time course images clearly show the migration pathway of the labeled MSCs (Fig.2, Panel A, B, C days 0,8,18 post QA injection respectively). The pathway is highlighted by the blue arrow (panel B only, for clarity), the QA injection site is highlighted by a green ellipse, and the MSCs deposition site is highlighted by a red circle (slice 1 only, for clarity). A closer look at the 100x100x75(µm)³ 3D GE images (Fig. 3) reveals that cells are found close to hyper-intense regions, where damage is probably more severe (yellow asterisks). The green circle again depicts the QA injection site and blue arrow depicts the migration pathway. Moreover, one animal that suffered cortical damage showed accumulation of the SPIO labeled cells in the cortex, implying that the cells can react to chemotactic signals derived from the lesion site, and find the paths to migrate towards it. Control animals exhibited no accumulation and no path of migration. Post-mortem histologic evaluation demonstrated that the distribution of the MSCs was comparable to the MRI images. Immunohistochemistry results show that phagocytosis has only partially occurred (CD68 positive), and that the cells maintained their differentiated identity (S100β positive).

Conclusions These findings show that in this experimental model of HD, the transplanted MSCs post differentiation to GF secreting cells, are viable for at least 18 days and can migrate to the most affected areas, and that MRI can be used to detect the paths of migration. This gives hope for future research on these cells, especially for the treatment of neuronal degeneration.

References: [1] Shwarcz R. et al., *Science* **219**: 316–318 (1983). [2] Lindvall O. et al., *Nature* **441**:1094-1096 (2006). [3] Bulte J. et al., *NMR Biomed.* **17**:484-499 (2004)

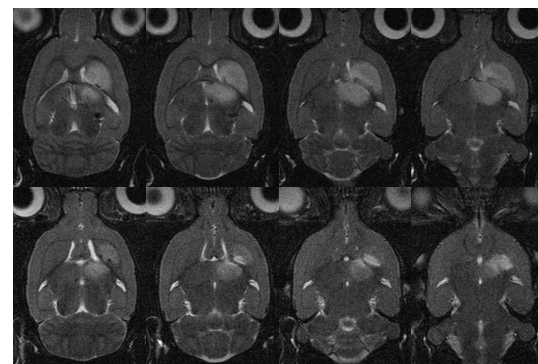


Fig. 1

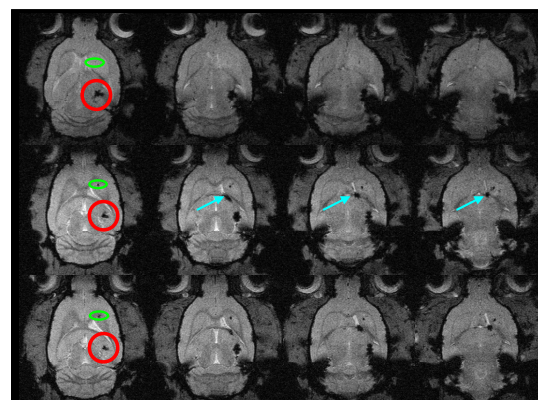


Fig. 2

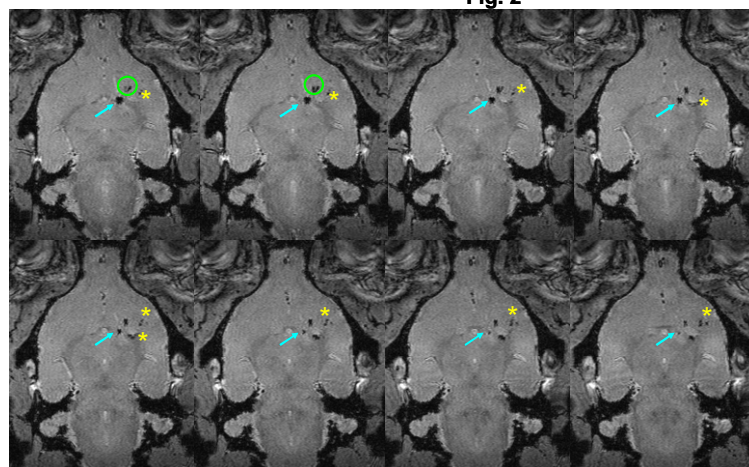


Fig. 3